Supporting Information

A Direct One-Step Synthetic Route to Pd-Pt Nanostructures with Controllable Shape, Size, and Composition for Electrocatalytic Applications

Youngjin Ye, Jin Joo, Seonggyu Lee, and Jinwoo Lee*

Corresponding author: jinwoo03@postech.ac.kr

Samples[a]	Pt-0	Pd_1Pt_5-0	Pd_1Pt_5-10	Pd_1Pt_5-19	Pd_1Pt_5-35	Pd_1Pt_5-45	Pd_1Pt_5-75
Average size (nm)	8.5	20.1	14.6	17.3	24.8	30.5	38.0
RSD (%)	40.8	31.3	19.7	18.8	17.7	14.1	18.8

Table S1. Average diameters and relative size distributions (RSDs) of Pt and Pd_1Pt_5 NCs.

[a] Numbers are the KBr concentrations (mM).

	Pd_2Pt_1-0	Pd_2Pt_1-75	Pd_2Pt_1-230	Pd_5Pt_1-0	Pd_5Pt_1-75	Pd_5Pt_1-230
Average size (nm)	9.1	18.8	23.0	9.0	9.4	16.2
RSD (%)	24.9	15.8	17.4	70.5	30.8	25.9

Table S2. Average diameters and relative size distributions (RSDs) of Pd_2Pt_1 and Pd_5Pt_1 NCs.

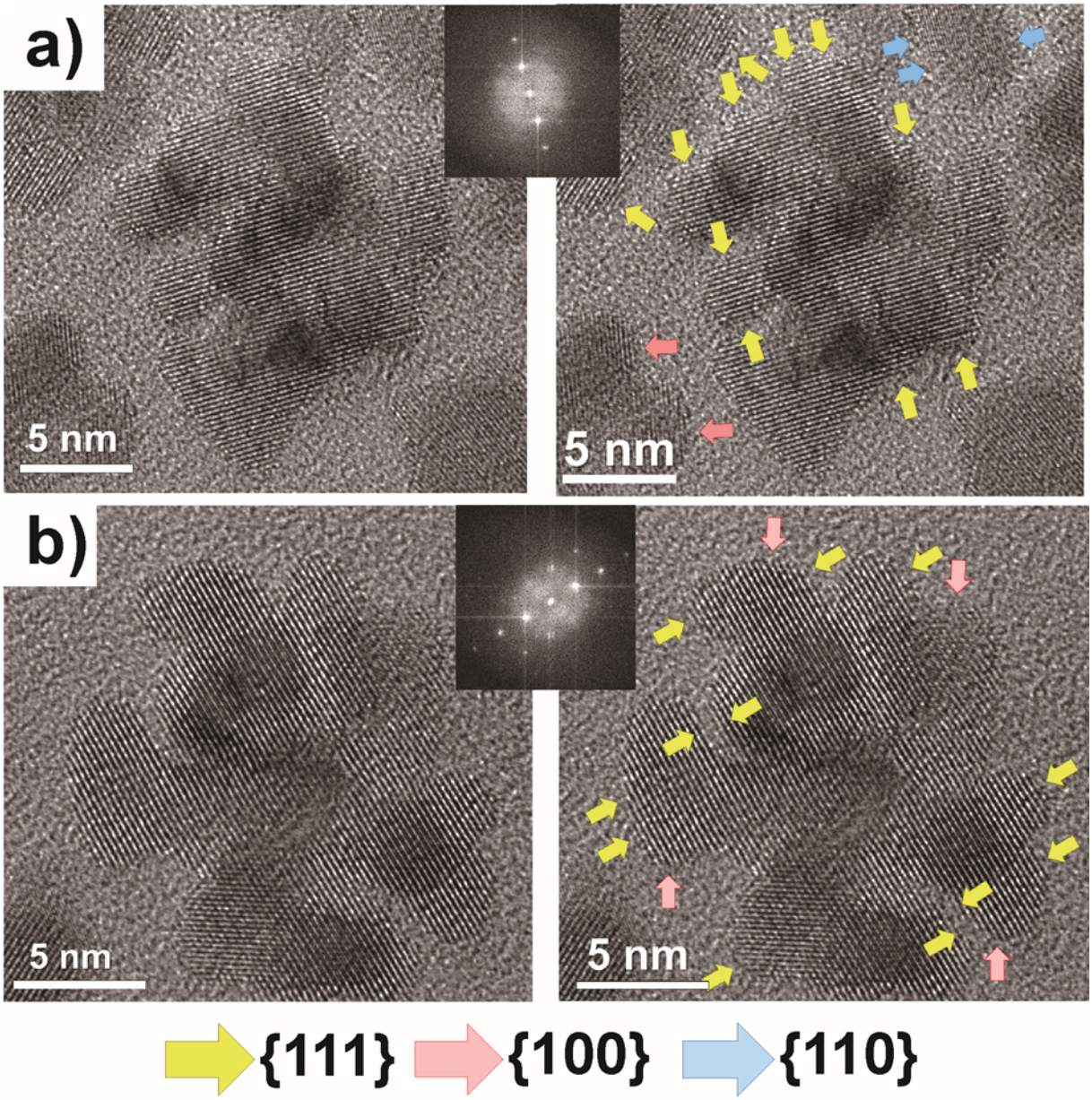

Fig. S1. HRTEM images of Pd_1Pt_5 dendrites and corresponding FFT patterns. Most of the exposed facets are {111} with some {100} and {110} facets.

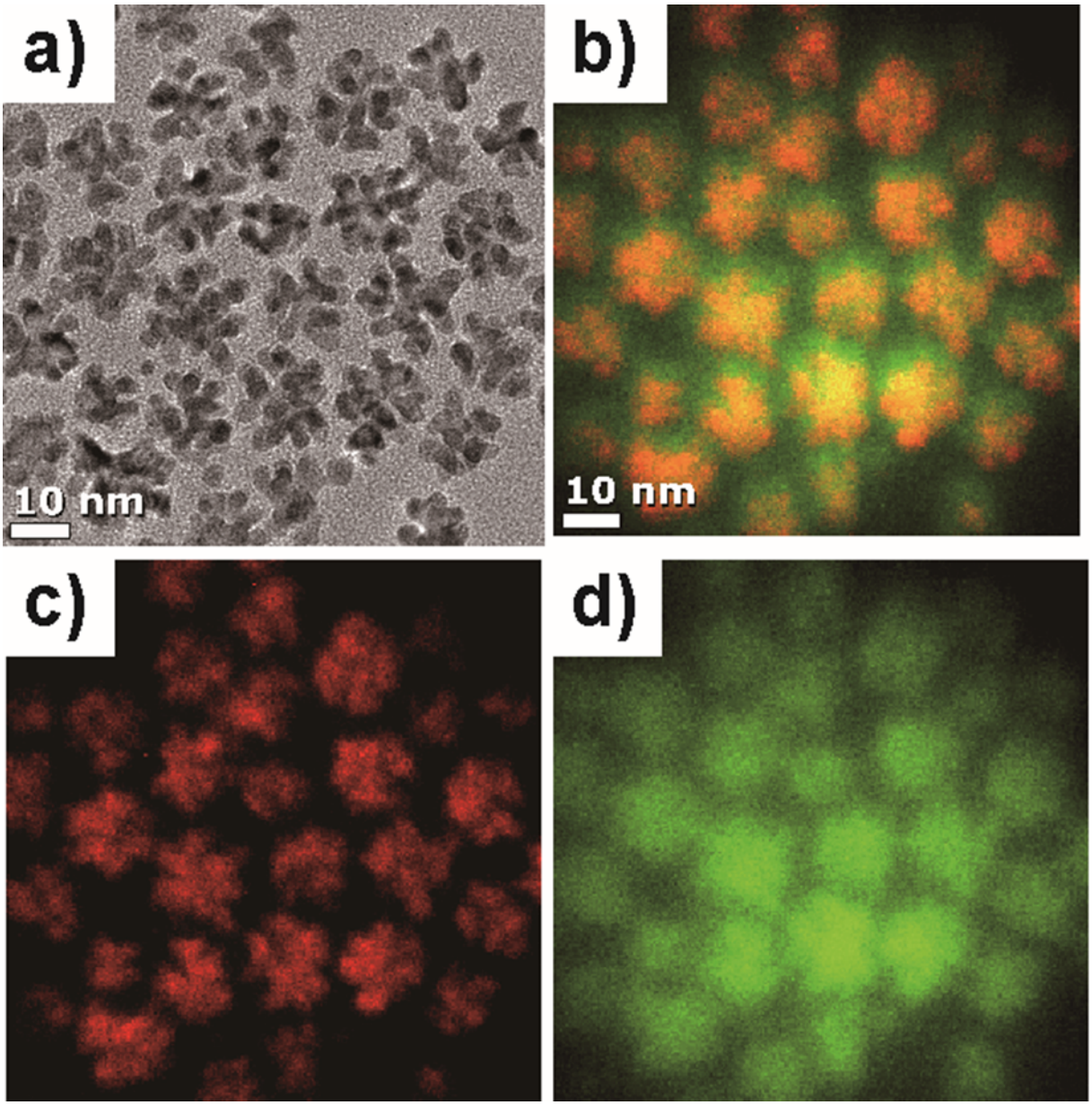

Fig. S2. (a) HRTEM image and (b-d) corresponding EELs mapping images of Pd_1Pt_5 dendrites. (b) Overlapped mapping images of Pd and Pt, and mapping images of (c) Pd and (d) Pt.

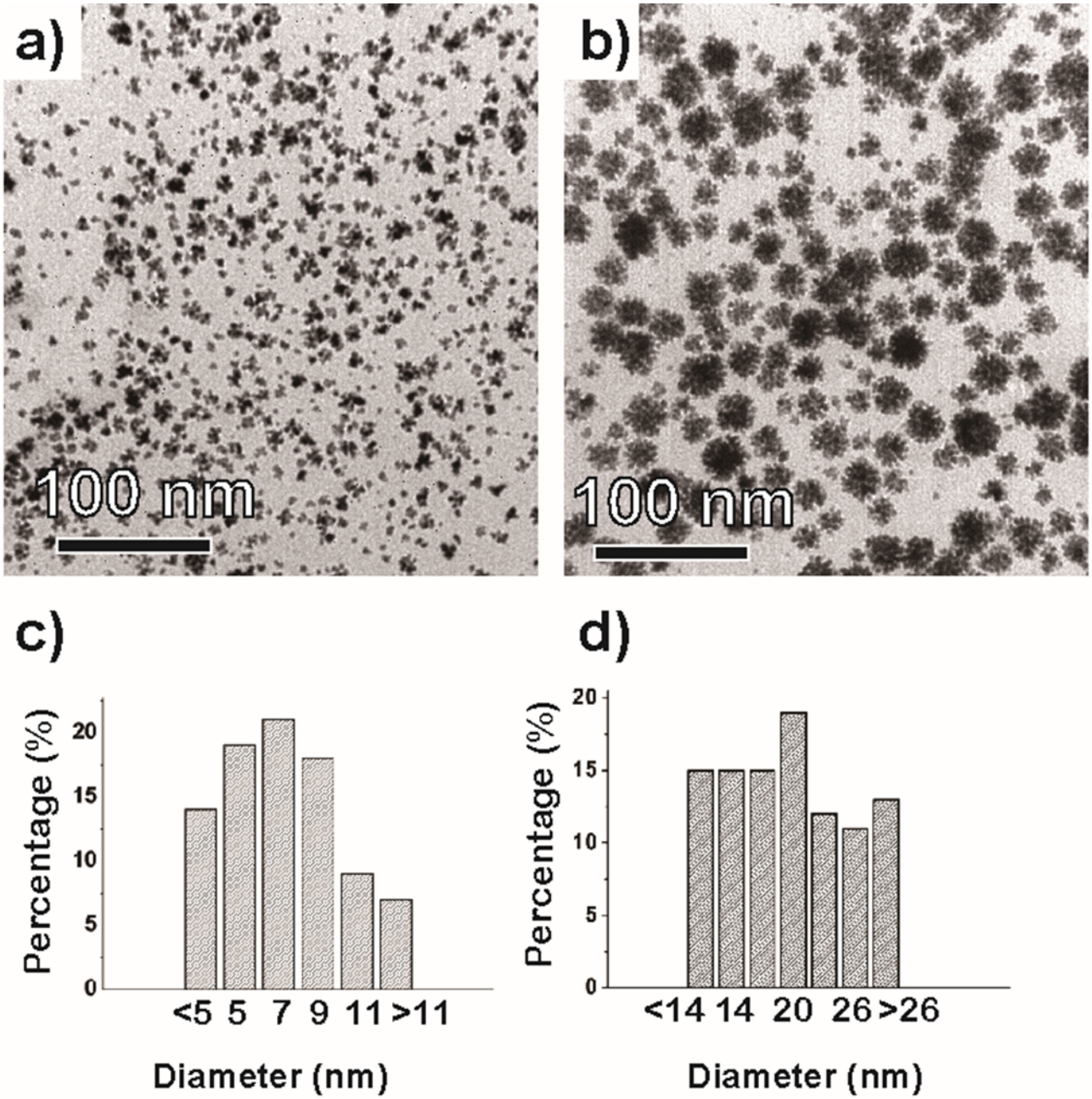

Fig. S3. (a) TEM image of Pt NCs prepared under the same condition as in Fig. 2a except that Na_2PdCl_4 was not used. (b) TEM images of Pd-Pt NCs prepared under the same condition as in Figure 1a except that KBr was not used. Size distributions of NCs in (c) Fig. S3a and (d) Fig. S3b.

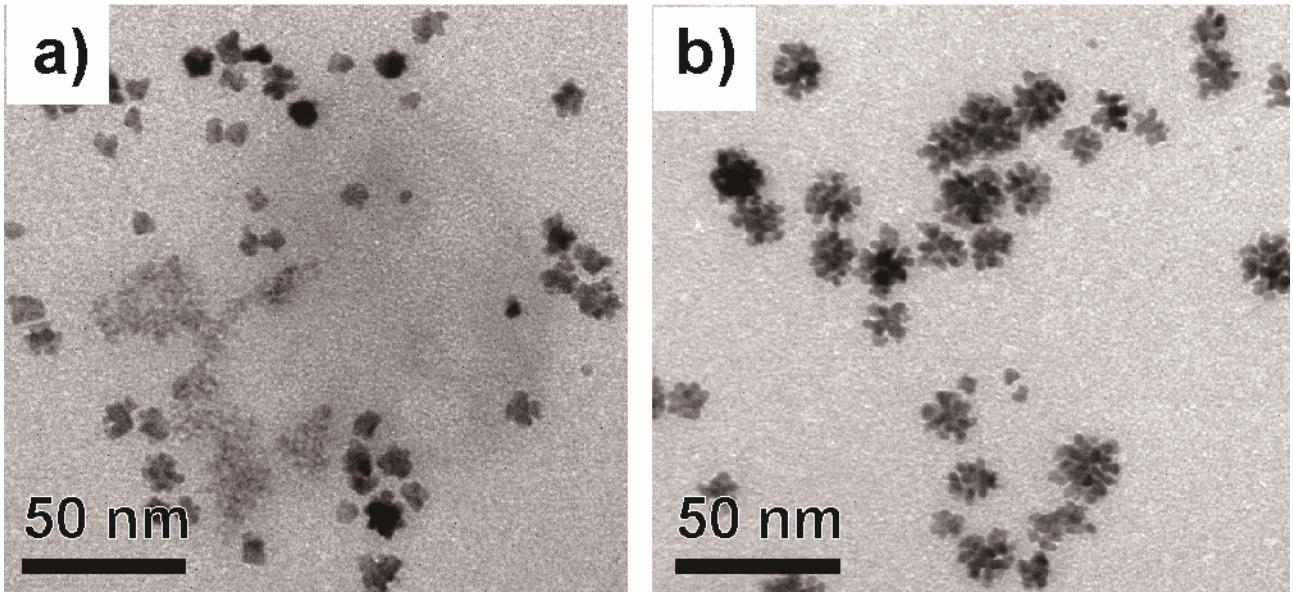

Fig. S4. TEM images of the Pd_1Pt_5 dendrites obtained after (a) 10 min and (b) 15 min.

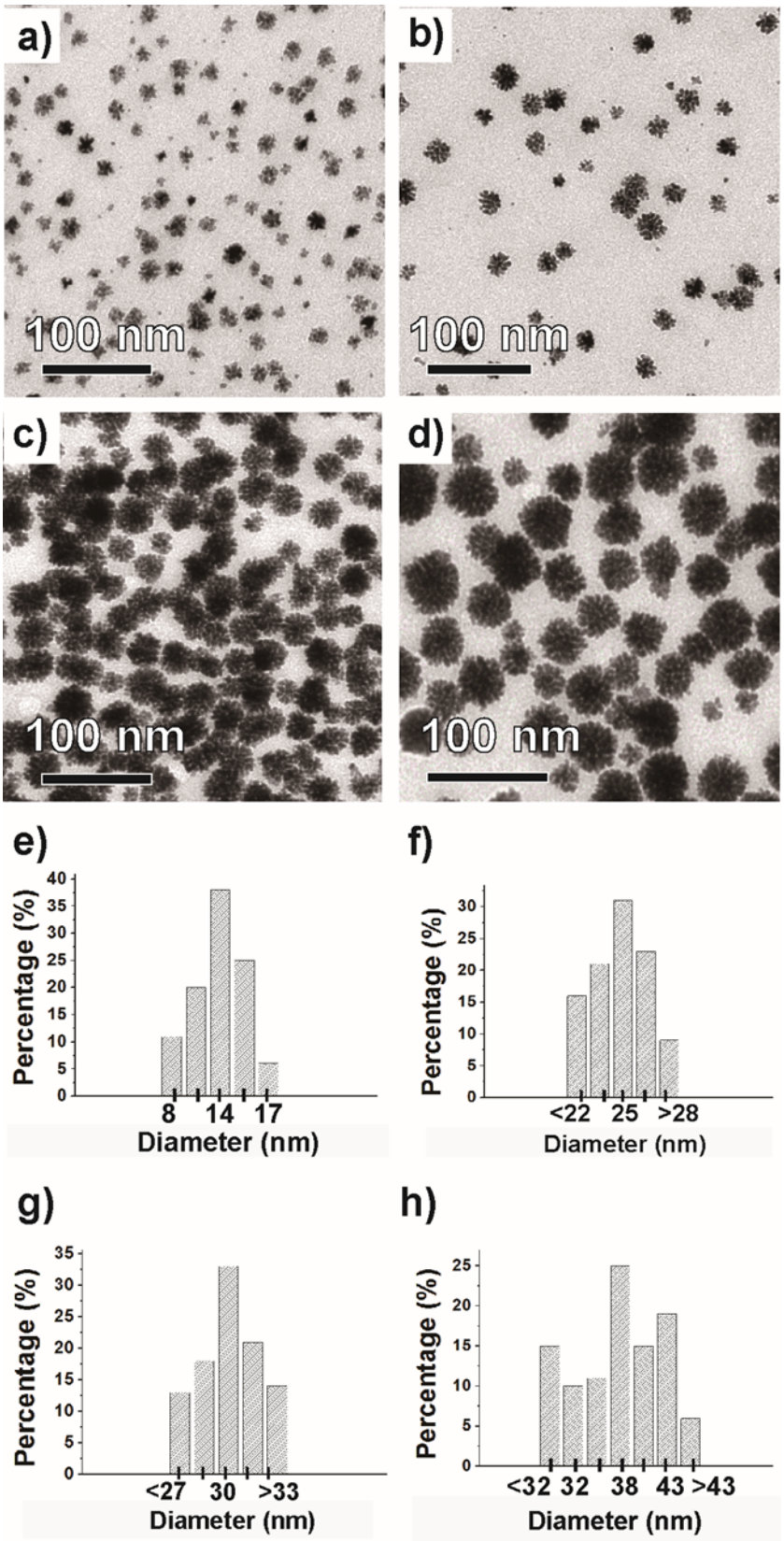

Fig. S5. Size distributions of Pt and Pd_1Pt_5 NCs which are shown in Fig. 3 in the manuscript.

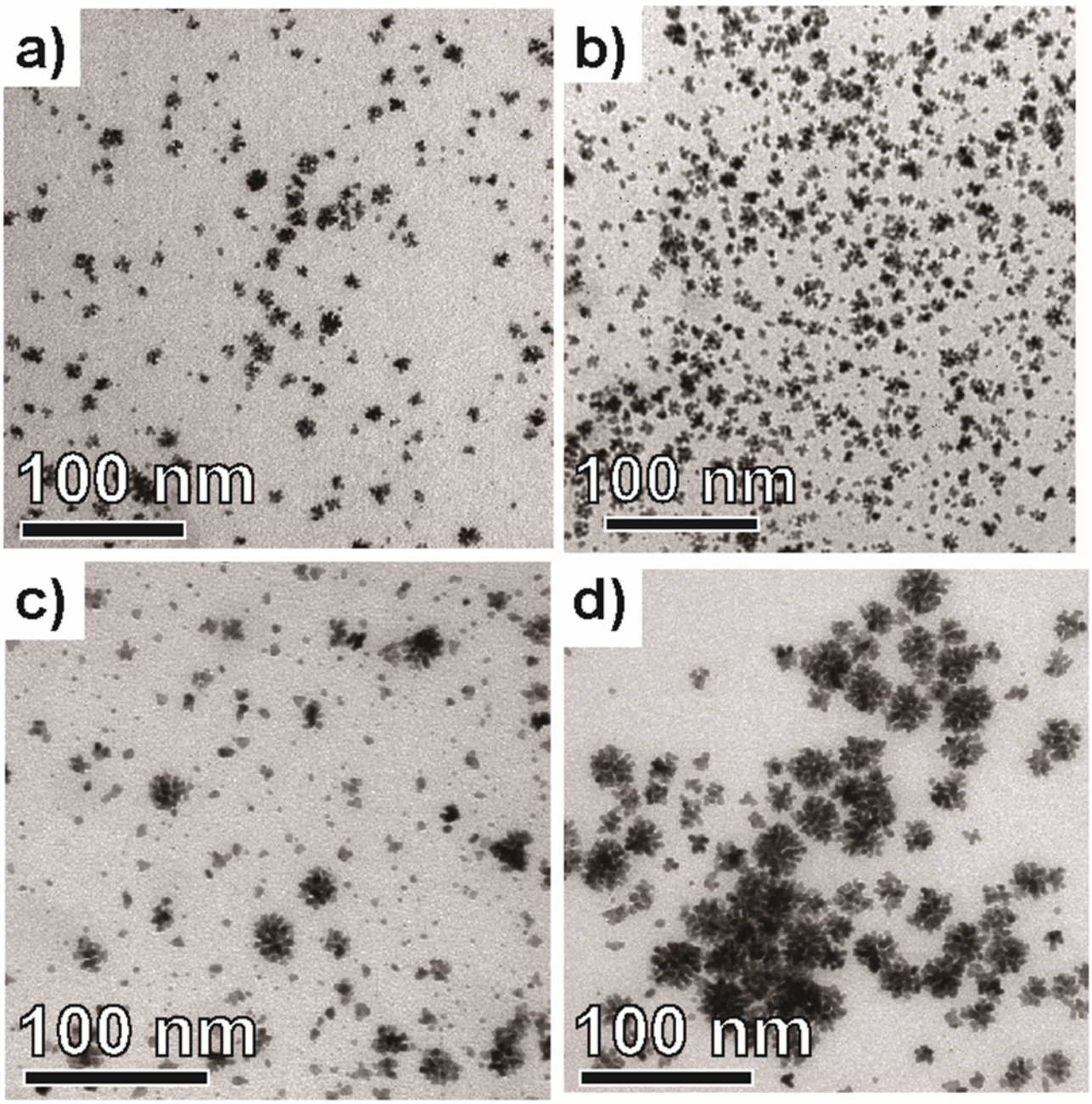

Fig. S6. TEM images of Pt NCs with varying KBr concentrations of (a) 0, (b) 19, (c) 60, and (d) 75 mM.

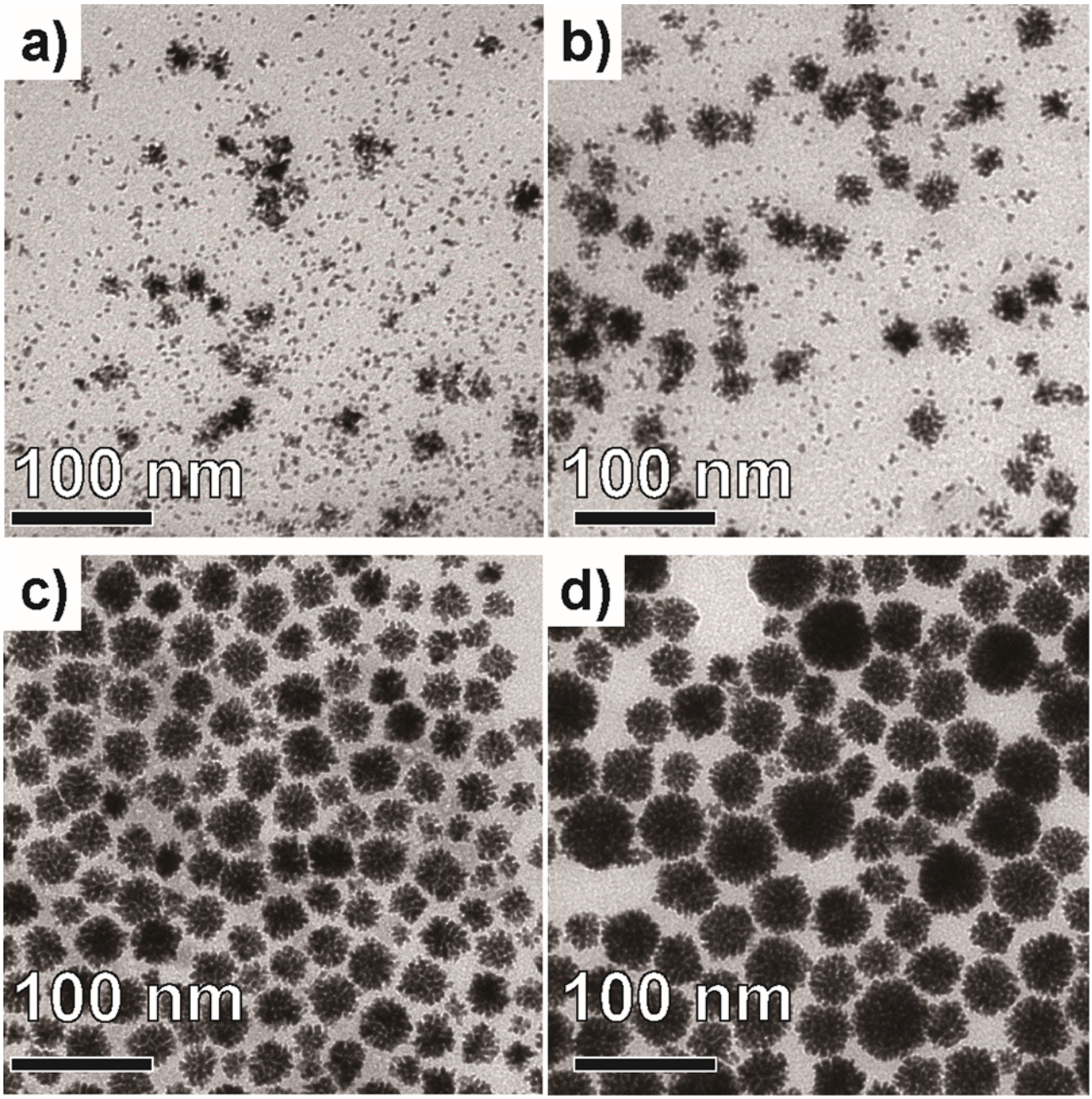

Fig. S7. TEM images of Pd_1Pt_5 NCs with different KCl/KBr molar ratios of (a) 9, (b) 4, (c) 1, and (d) 0.4.

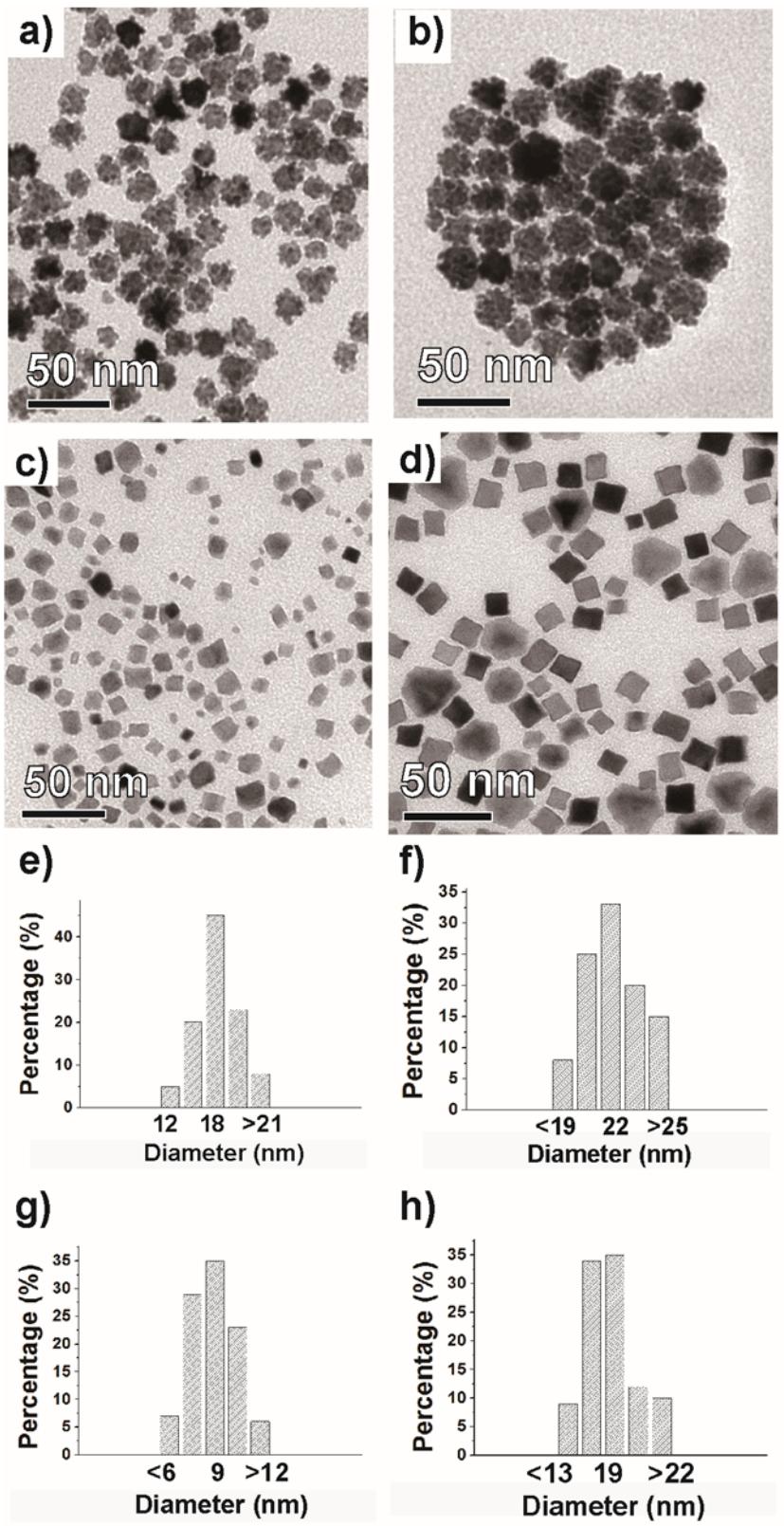

Fig. S8. Size distributions of Pd_2Pt_1 and $Pd_{10}Pt_1$ NCs which are shown in Fig. 4 in the manuscript.

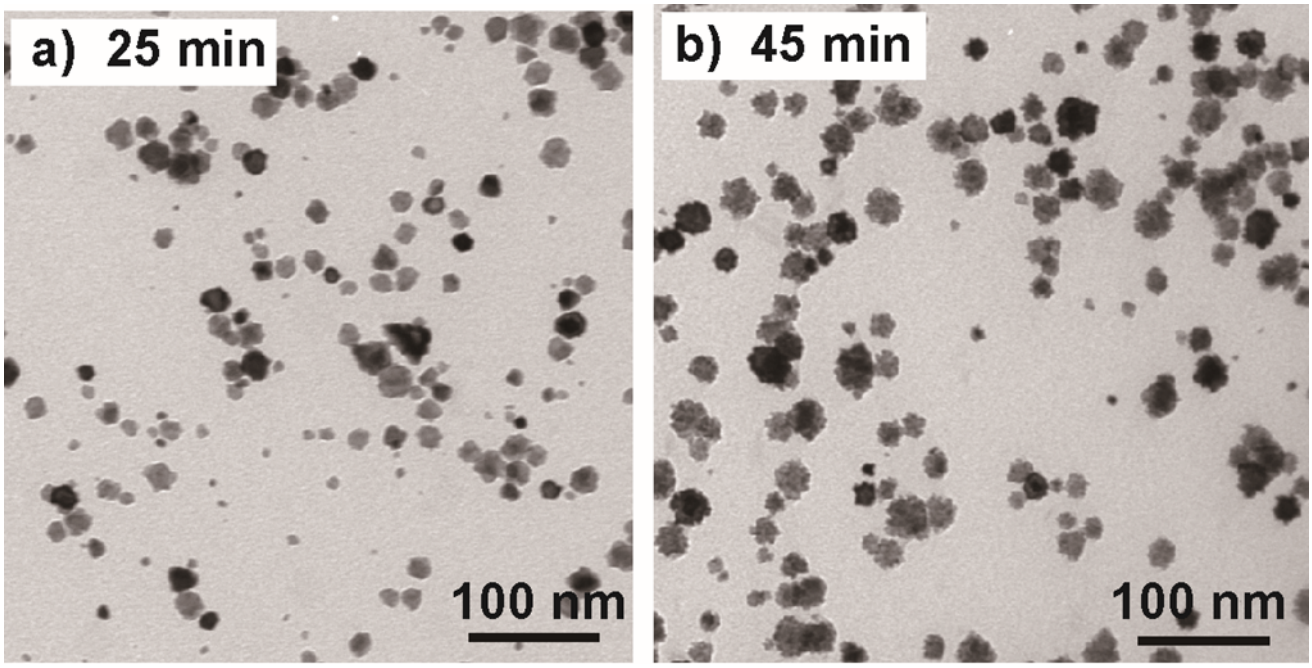

Fig. S9. TEM images of Pd_2Pt_1 NCs with KBr concentrations 230 mM, obtained after (a) 25 min and (b) 45 min.

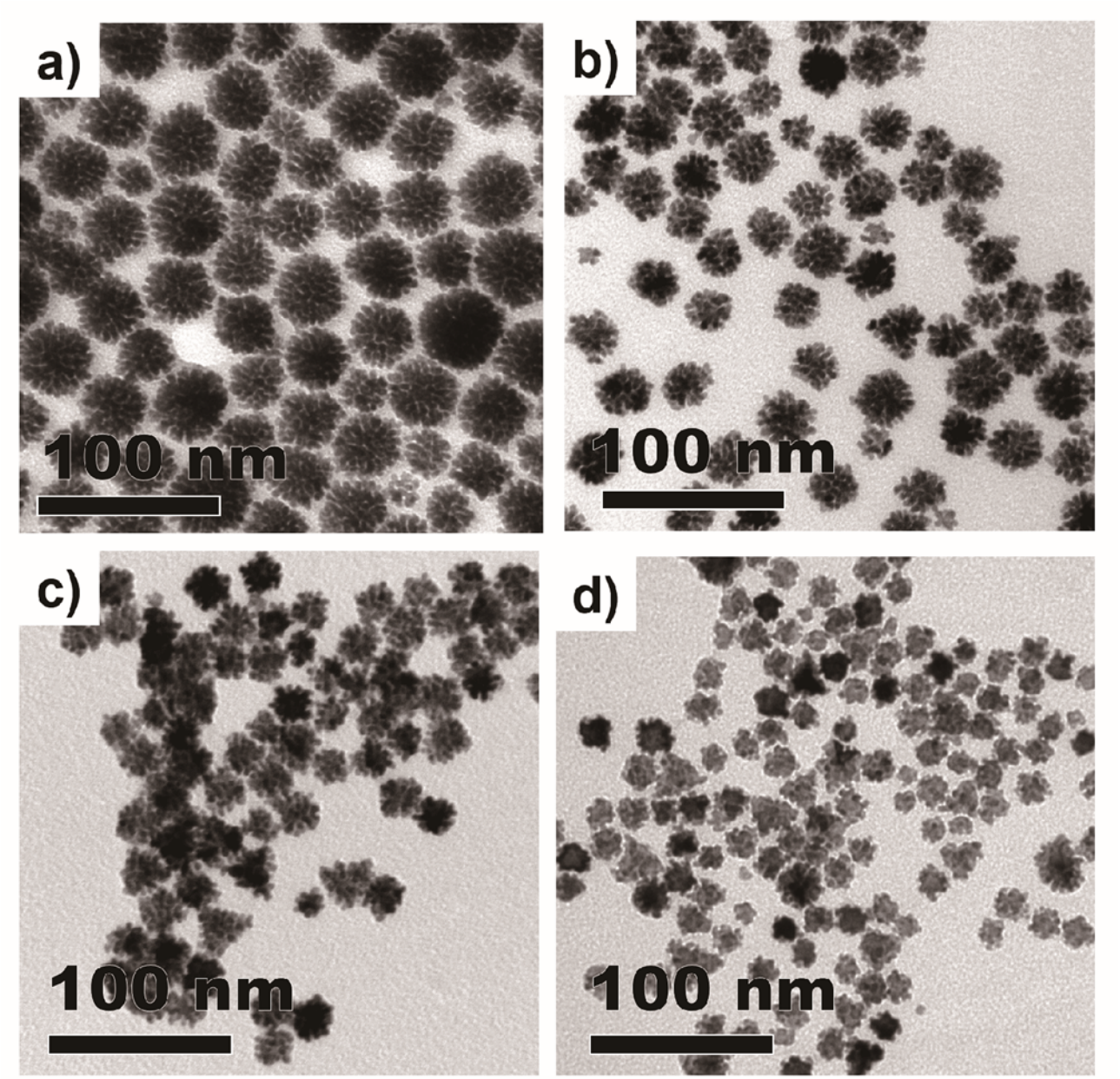

Fig. S10. TEM images of Pd-Pt NCs with different compositions, which were synthesized at 75 mM of KBr concentration; (a) Pd_1Pt_5, (b) Pd_1Pt_2, (c) Pd_1Pt_1, (d) Pd_2Pt_1.

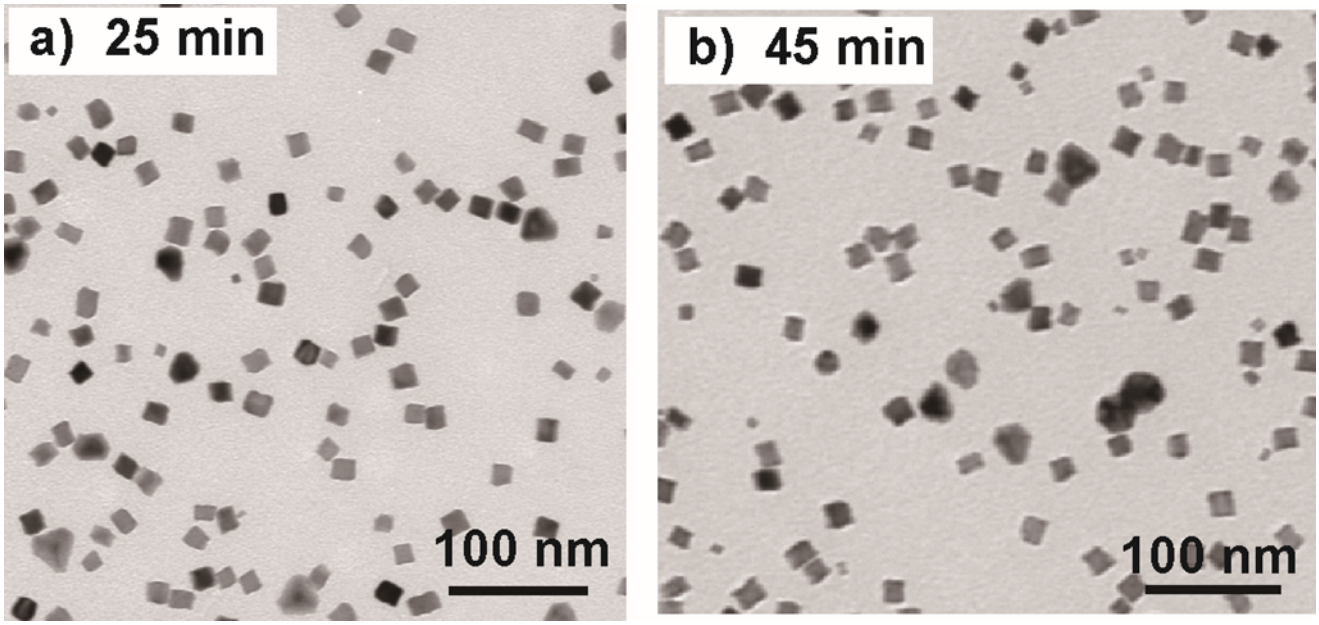

Fig. S11. TEM images of $Pd_{10}Pt_1$ NCs with KBr concentrations 230 mM, obtained after (a) 25 min and (b) 45 min.

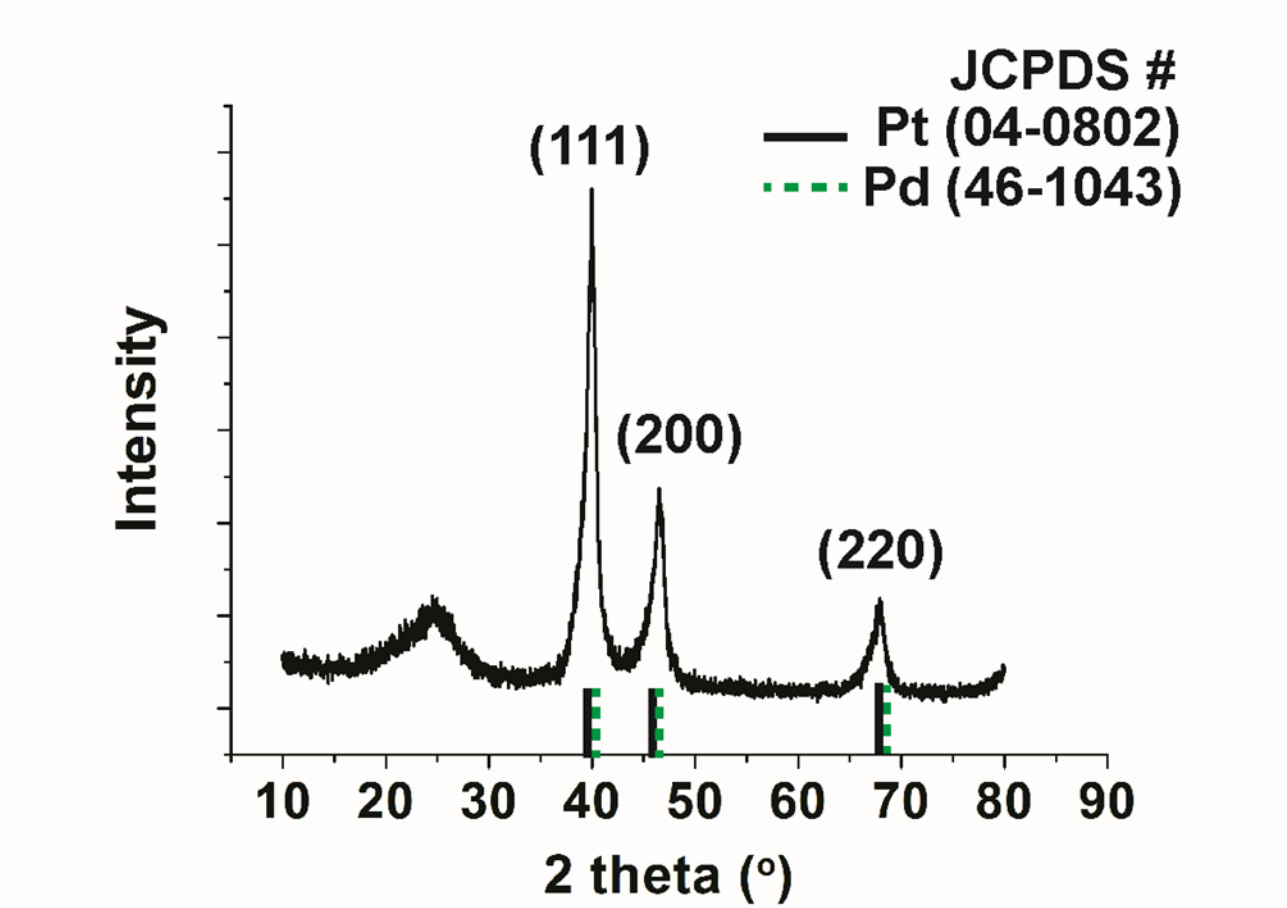

Fig. S12. XRD patterns of Pd_1Pt_5 dendrites supported on carbon black.

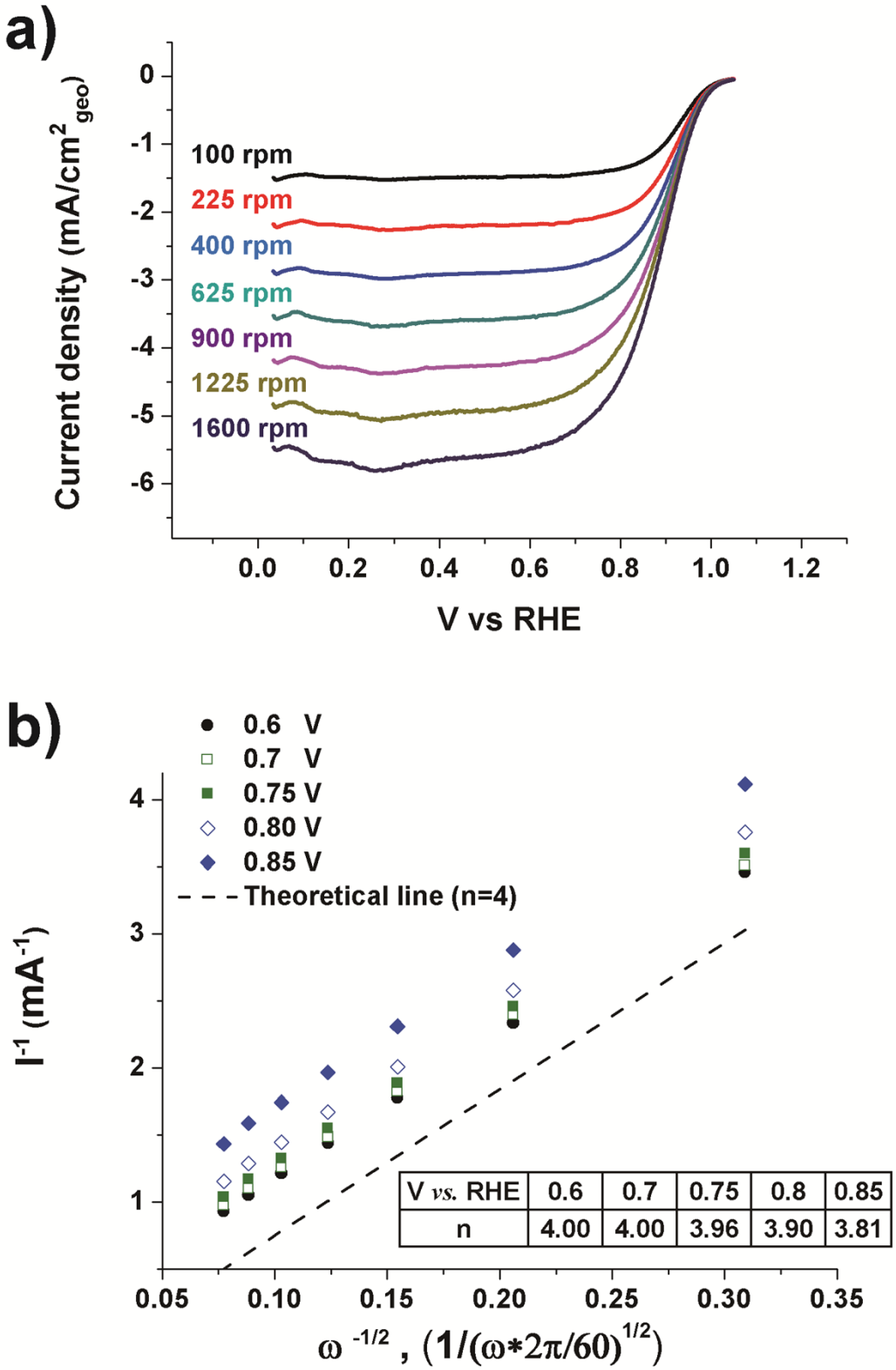

V *vs.* RHE	0.6	0.7	0.75	0.8	0.85
n	4.00	4.00	3.96	3.90	3.81

Fig. S13. (a) Polarization curves for ORR on a Pd_1Pt_5/C in a 0.1 M $HClO_4$ solution with a sweep rate of 20 mV s^{-1}. (b) Koutecky-Levich plots for Pd_1Pt_5/C at various potentials. The inset table shows the electron transfer numbers at various potentials.

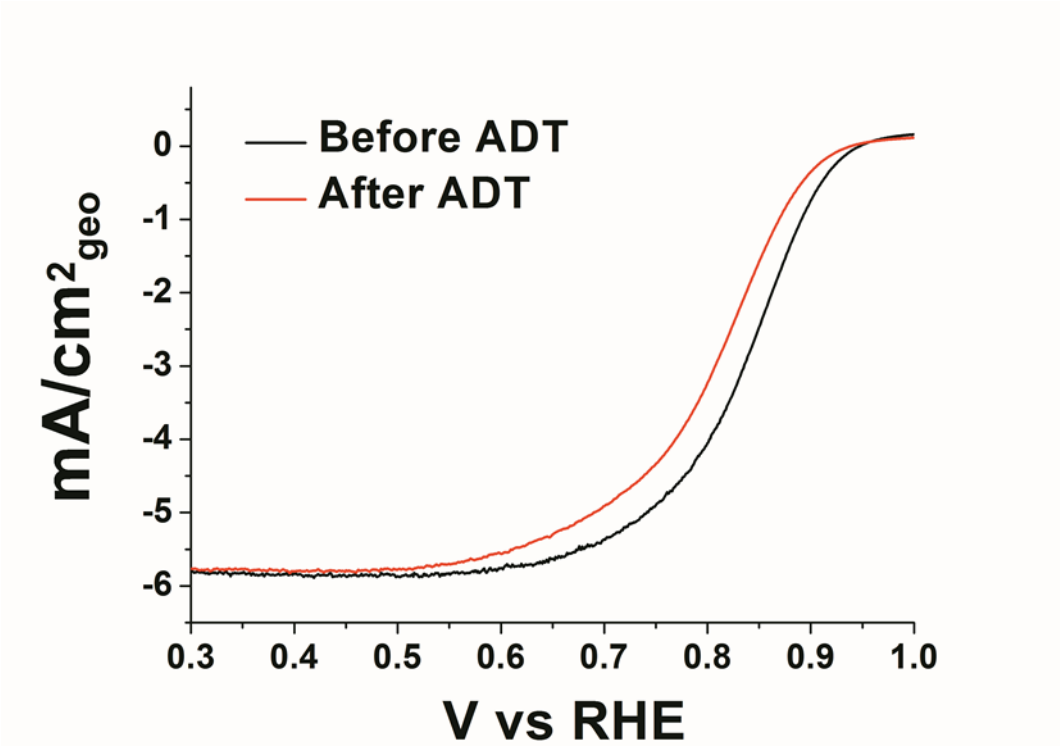

Fig. S14. ORR polarization curves of Pt/C before and after the ADT.

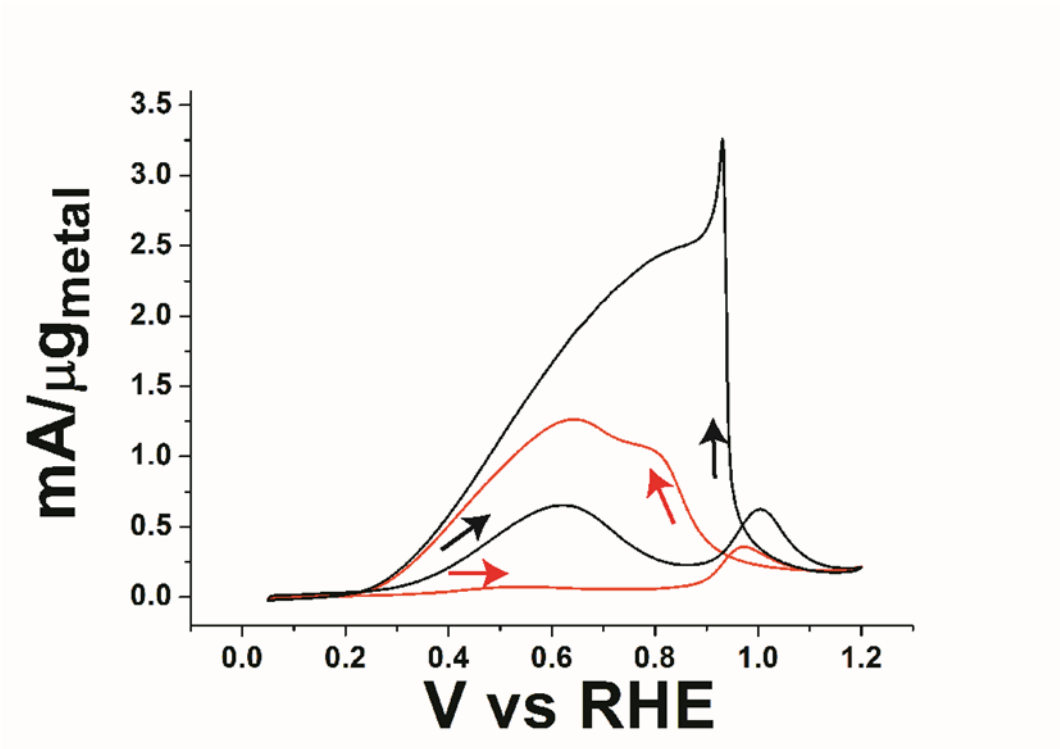

Fig. S15. FAOR polarization curves of Pd_1Pt_5/C (black) and Pt/C (red), which show both forward and backward sweeps.